ELSEVIER

Materials Characterization xx (2006) xxx–xxx

MATERIALS CHARACTERIZATION

Calculating the elastic modulus from nanoindentation and microindentation reload curves

David J. Shuman [a,*], André L.M. Costa [b], Margareth S. Andrade [a]

[a] *Metallurgical Technology Division, Fundação Centro Tecnológico de Minas Gerais, Av. José Cândido da Silveira 2000, CEP 31170-000, Belo Horizonte, MG, Brazil*

[b] *Department of Materials Engineering, Universidade Federal do Pará, Folha 17, quadra 4, lote especial, CEP 68513-480, Marabá, PA, Brazil*

Received 3 June 2005; received in revised form 8 June 2006; accepted 8 June 2006

Abstract

The Oliver–Pharr method was used to calculate the elastic modulus from the reloading curve and was compared to the traditional unloading curve method. Nanoindentation and microindentation testing instruments were used. This method was applied to load–unload–reload–unload, multistep, and cycle indentation testing procedures at various hold times and force rates. On unloading the reverse plasticity added to the elastic recovery which increased the apparent elastic modulus. During reloading there was mainly elastic deformation making it more reliable for the elastic modulus calculation. It was also found that the metals tested started yielding between 70% and 100% of the reload curve. The reload indentation elastic modulus for fused silica and several metals was equivalent to the tensile test elastic modulus from reference literature.

Keywords: Nanoindentation; Microindentation; Elastic modulus; Reload curve; Metals

1. Introduction

There is a large interest and many advantages in measuring the elastic modulus of small size samples and microstructural features. For example less sample material is needed for indentation testing than it takes to make a tensile tester bar. Sometimes it is desirable to measure the mechanical properties of each component of a composite or multiphase material. In either case the elastic modulus can be measured by using a device called instrumented indentation tester (IIT) also known by several other names such as a depth sensing indentation (DSI) tester, dynamic hardness tester, nanoindenter, microindenter, or even macroindenter. To measure the indentation elastic modulus the instrument must digitally record the displacement and force during the indentation process. The slope of the unload curve has commonly been used to calculate the elastic modulus. Two of the most commonly used unload curve analysis techniques are the Doerner–Nix [1] and Oliver–Pharr [2] methods.

The nanoindentation technique has had widespread success measuring the mechanical properties of thin-films. However, when either of these analysis techniques is used to measure the elastic modulus of metals the results are far from the actual tensile-test values. Doerner and Nix [1] had measured 480 GPa for tungsten using

* Corresponding author. Tel.: +55 31 3489 2355; fax: +55 31 3489 2200.

E-mail address: djshuman@yahoo.com (D.J. Shuman).

1044-5803/$ - see front matter © 2006 Elsevier Inc. All rights reserved.
doi:10.1016/j.matchar.2006.06.005

nanoindentation whereas the known modulus is 420 GPa. Rodríguez and Gutierrez [3] found that aluminum had an indentation elastic modulus of over 80 GPa whereas the known elastic modulus is 70 GPa. Garrido Maneiro and Rodríguez [4] did a study of the nanoindentation with spherical–conical tips and observed an increasing elastic modulus with an increasing load for two aluminum alloys. This inflated elastic modulus value for metals is often attributed to the indentation pile-up, the indent size effect and elastic recovery [5]. The indentation test is similar to a compression test and the stress under an indenter is different than that in a round or flat bar in tension. Also the lateral displacement of material at the free surface around the edge of the indenter means that a uniaxial stress field is not maintained during unloading. On the other hand, non-metallic materials, such as fused silica, soda-lime glass, and silicon, do not form pile-up during indentation and therefore the unload curve provides good results of elastic modulus [2].

Multistep indentation tests can be used to measure the elastic modulus at various depths from a single indent. The benefit of multistep testing is that more information about the material can be collected in a shorter time because each step has an unload and a reload curve. The test results from a multistep indentation are more homogenous than placing single indentations at various locations on the sample surface. For example when individual indentations are placed into a polycrystalline material each indent is placed inside a grain of different orientation. For the multistep tests the grain orientation is fixed relative to the indenter. However, as the depth of the indentation increases for each step there is an increased interaction with the surrounding grains.

The load–unload–reload–unload, multistep and cycle tests have both unloading and reloading curves. The beginning of the reload curve would logically have less influence on the pile-up because it starts in the bottom portion of the indentation. Also it will have a uniaxial stress field because it is far from the free surface. A pyramidal tip indenting the material creates a complex stress field. Finite element simulation of indentations into elastic-plastic materials predicts that the reload curve should follow the same path as the unload curve [6]. However, some materials are known to experience reverse plasticity [2] or reversible phase transition [7]. In both cases an unload–reload hysteresis loop is observed. The physical meaning of reverse plasticity is still unclear but it seems to be the difference in load-displacement response between the ideal elastic behavior to what is actually observed.

For metals it is unclear what physically occurs during unloading and reloading. If both the unload or reload curves have the same slope they should give the same elastic modulus calculation assuming that the contact mechanics of the unloading exactly equals the reloading. For metals there might be stress relaxation reverse plasticity during unload that does not exist for reloading. This would influence the final elastic modulus calculation. In this research unload and reload curves were studied in an attempt to understand and improve the nanoindentation and microindentation elastic modulus measurement accuracy for metals.

2. Materials and methods

2.1. Theoretical approach

Fig. 1 shows a schematic of an indentation load-displacement curve. A power law curve was fit to the unload data points. This curve was extrapolated to the fully unload final indentation depth. The slope S at the maximum load data point is used to calculate the elastic modulus. Refer to this schematic to help understand each of the terms presented below.

The elastic modulus of materials is calculated from the unload or reload curve by using the following Eqs. (1)–(7). Eq. (1) was derived from the Hertzian theory of contact mechanics [8].

$$E_r = \frac{\sqrt{\pi}}{2} \cdot \frac{S}{\sqrt{A_p}} \tag{1}$$

where A_p is the projected area of contact and S is the slope of the unload at the maximum displacement point (h_{max}). The reduced modulus E_r is a combination of the sample material and indenter elastic deformations. In

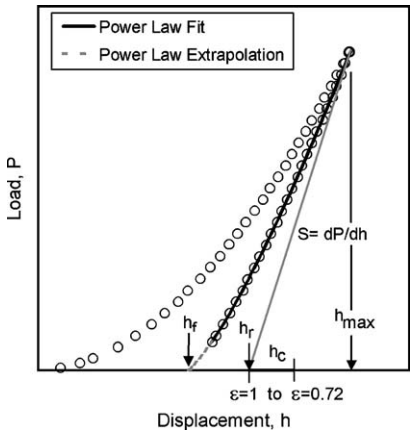

Fig. 1. Schematic representation of a typical load-displacement curve from an instrumented indentation tester including the power law fit and several key points.

order to separate the indenter elastic deformation contribution from the sample material elastic modulus Eq. (2) was used:

$$E = \frac{1-v_s^2}{\frac{1}{E_r} - \frac{1-v_i^2}{E_i}} \tag{2}$$

where the E and v are the elastic modulus and Poisson's ratio of the sample material, and E_i and v_i are for the indenter.

The Hertzian method requires knowing the projected contact area at the maximum load. The ideal projected area function A_p for a Berkovich indenter is $A_p = 24.56\ h_c^2$, where h_c is the contact depth during indentation full load. However, at nanoscale and microscale depths the tip radius must also be considered. Thus, a two-term equation was used for the projected area function, where the first term C_0, and the second term C_1 were adjusted to account for the tip rounding [9].

$$A_p = C_0 h_c^2 + C_1 h_c \tag{3}$$

The indentation contact depth h_c is not equal to the total displacement h_{max} of the indenter into the sample because the surrounding surface deforms elastically during unloading. According to the Doerner–Nix and the Oliver–Pharr analysis methods, h_c can be calculated by:

$$h_c = h_{max} - \varepsilon(h_{max} - h_r) \tag{4}$$

$$h_r = h_{max} - (P_{max}/S) \tag{5}$$

where P_{max} is the maximum load, h_r is where the unload curve slope intersects with the displacement axis (see Fig. 1) and ε is the Sneddon's correction factor for the contact depth that takes into account the indenter geometry influence on sample deformation. The Sneddon's coefficient ε can vary from 0 to 1 and is equal to 1 for a flat punch and 0.72 for a Vickers indenter. Experiments have shown that for the Berkovich indenter ε can be between 0.72 and 0.78 [10,11].

Currently the most accepted analysis method for calculating the slope of the unload curve at the maximum displacement is the Oliver–Pharr method [2]. Their approach assumes that the unload curve is conveniently described by a power-law:

$$P = \alpha(h_{max} - h_f)^m \tag{6}$$

The above equation is non-linear and a numerical analysis technique is required to solve for α, m and h_f. The α and m are constants and h_f is the final residual indent depth. Usually between 25% and 100% of the unload curve data are commonly used for the fitting function depending on the quality of the data [10]. The slope S at the maximum displacement data point h_{max} is calculated by taking the first derivative of Eq. (6) as:

$$S = dP/dh = \alpha m(h_{max} - h_f)^{(m-1)} \tag{7}$$

Eqs. (1)–(7) were combined to make a single equation to conveniently calculate the sample elastic modulus E. The only term that needs to be assumed is the sample Poisson's ratio v_s.

$$E = \frac{(1-v_s^2)}{\frac{2\sqrt{C_0 \cdot h_c^2 + C_1 \cdot h_c}}{a \cdot m(h_{max} - h_f)^{m-1} \cdot \sqrt{\pi}} - \frac{(1-v_i^2)}{E_i}} \tag{8}$$

2.2. Materials

The materials tested were fused silica, AA5050-O aluminum, AISI 1020 steel, iron, electrolytic copper and electrolytic nickel. Chemical analysis was performed on the aluminum and steel samples to confirm the alloy type. The Poisson's ratio used for each of the materials was 0.17 for fused silica [2], 0.29 for the iron and steel [12], 0.33 for aluminum, 0.31 for nickel, and 0.35 for copper [13]. Each of the metals was prepared using the same metallographic procedure. They were mechanically polished using SiC wet sandpaper, suspended diamond particles, and then a final polishing step for 5 min using Struers OP-S. The fused silica was purchased with an optically flat surface.

2.3. Experimental procedure

Various indentation tests were done to compare the elastic modulus from the reload curve to the unload curve. Fig. 2 shows a schematic of the three types of tests that were used: load–unload–reload–unload, cycles, and multistep. For all of these testing procedures there is both an unload and a reload curve after the initial loading. In the cycle tests the same force is applied several times to the indenter while for multistep tests the load was increased after each unload/reload cycle.

The experimental devices used for indentation testing were a Shimadzu DUH-W201S dynamic ultra-micro hardness tester and a MTS Nanoindenter XP. Both machines create the indentation force by sending an electric current through an electromagnetic coil producing

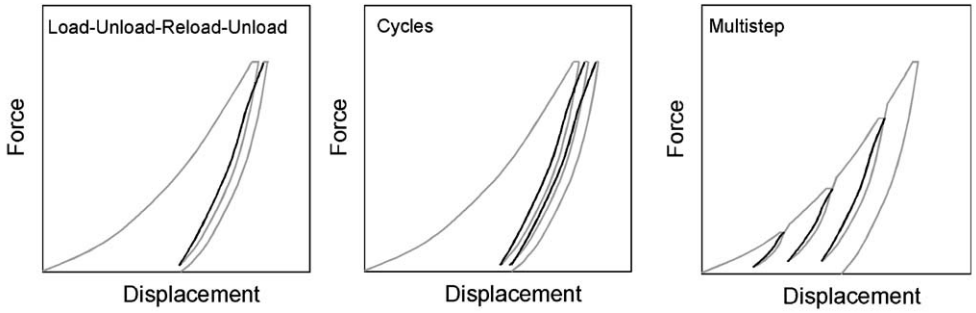

Fig. 2. Schematic representation of the load–unload–reload–unload, cycle, and multistep indentation testing procedures. The reload section is shown as a dark curve in each of the graphs.

a magnetic field, which applies the force and displacement onto the indenter. The Nanoindenter XP applies the force using a calibrated electromagnetic coil with a resolution of 50 nN. Because of its design the Nanoindenter XP produced reliable measurements in the nanodisplacement range. A diamond Berkovich indenter was used to make the indentations in both testing instruments. Diamond indenters have an elastic modulus of 1141 GPa and Poisson's ratio of 0.07 [2].

Prior to indentation testing the instrument frame-compliance and indenter area function were found using the Oliver–Pharr method with fused silica [2]. The frame-compliance of the DUH-W201S was Cf=0.24 nm/mN and the indenter area function was A_p (nm^2)=24.5 h_c^2+1500 h_c. The Nanoindenter XP frame-compliance was negligible because the instrument was pre-calibrated by the manufacturer and its indenter area function was determined as A_p (nm^2)=28.1 h_c^2+1600 h_c. The laboratory testing conditions for both instruments was approximately the same: room temperature and relative humidity between 65% and 70%.

Load–unload–reload–unload and multistep tests were done using the DUH-W201S microindenter over a range of 50 to 700 mN. The multistep parameters were set to 10 steps. The first step started at 70 mN and increased by adding 70 mN until the maximum force of 700 mN was reached. The constant applied force rates were 7.10, 23.5, and 70.6 mN/s with hold times of 1, 5, and 15 s. This instrument repeated the hold time at the minimum force of each unload cycle. For the single load–unload–reload–unload test forces of 50, 100, 200, 300, 400, 500, 600, and 700 mN were used with a constant applied force rate of 23.5 mN/s and a hold time of 5 s. After each test the binary raw data files were converted into ASCII text files.

The same fused silica, copper, and steel samples were tested using the Nanoindenter XP. Multistep and cycle tests were performed. For multistep tests the first step started at 1.25 mN and was doubled 9 times until the final load of 320 mN was reached. The Nanoindenter XP was set to a constant displacement rate of 10 nm/s with a top hold time of 15 s. Cycle tests were done to see if the elastic modulus changes with an increasing number of cycles. The Nanoindenter XP was programmed to make 20 cycles at the forces of 50 and 400 mN, again with a constant displacement rate of 10 nm/s and a hold time of 15 s. The Nanoindenter XP indentation curves were saved as ASCII text files.

Experimental C++ software called Dureza was made to analyze the vast amount of curve data that was quick, automatic, documented and reproducible. It was programmed to calculate the elastic modulus using the Oliver–Pharr method [2]. The entire unload or reload curve data (100% of the points) was used for the non-linear numerical power-law fit. The Sneddon's contact depth correction factor was set to ε=0.78. The experimental software automatically separated multistep and cycle data into individual unload and reload curve text files. The hold time data was eliminated. The unload curve started after the top hold time and ended at the beginning

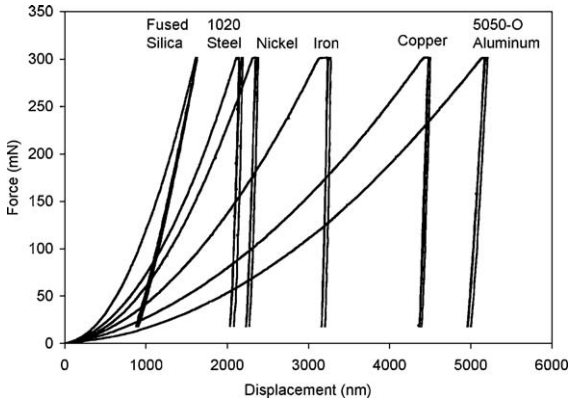

Fig. 3. Load–unload–reload–unload curves for various materials obtained with the Shimadzu tester using a constant applied force rate of 23.5 mN/s and a hold time of 5 s.

of the bottom hold time. The reload curve started after the bottom hold time and went up to the previous unload maximum force.

3. Results

Fig. 3 shows basic load–unload–reload–unload curves for each of the materials tested. The fused silica, shown on the left side, is the hardest material and aluminum; on the right side, is the softest. The first and the second unload curves overlap for the fused silica as shown by the small spacing between them. The metals had a greater displacement of the second unload curve because of a creep. Each material had a slightly different amount of creep displacement at the maximum force hold time. Fused silica had the least amount of creep and iron had the most. This creep was most likely caused by dislocation motion because all samples were tested at room temperature, which was below half the melting point. It was also observed in Fig. 3 that the fused silica unload and reload curves had apparently the same slope. The

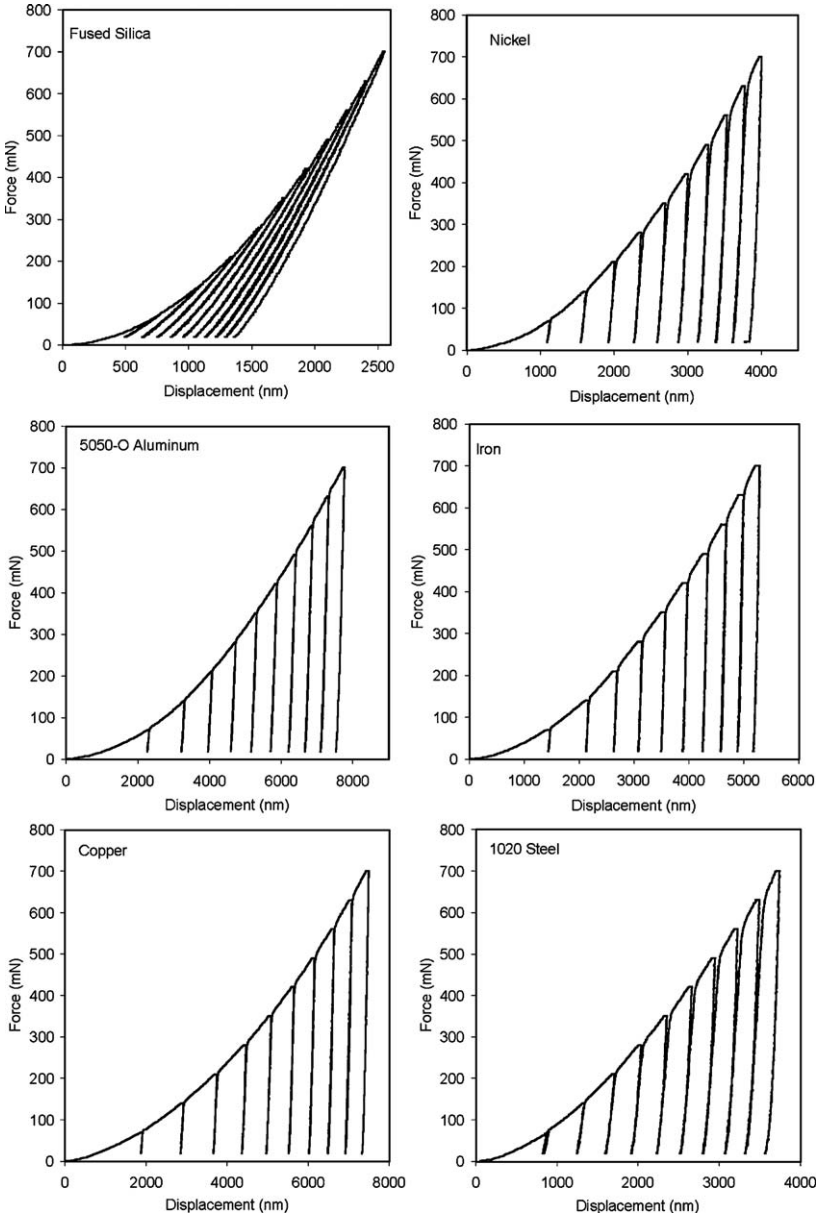

Fig. 4. Multistep microindentation tests for different materials using the Shimadzu instrument with a constant force rate of 23.5 mN/s and a hold time of 5 s.

metals had nearly a vertical slope during unload with only a small difference between the maximum and final depth. The materials with the greatest elastic recovery were fused silica and secondly aluminum.

Fig. 4 shows the multistep microindentation curves for each of the materials obtained at a constant force rate of 23.5 mN/s and a hold time of 15 s. The tests done at the other force rates and hold times presented similar curves but the metals presented less creep displacement for the shorter hold times. The fused silica did not have plastic deformation at the maximum load hold time. The nickel, iron, and steel samples had a clear step like feature at the top hold time apparently caused by the previously discussed creep. On the nickel and steel multistep curves there was a gap between the unload and reload curves that started at about 75% of the previous maximum load. This indicates that these materials began yielding before reaching the previous maximum load. The fused silica and the other metals did not present a significant gap at the top of the reload curve. A hold

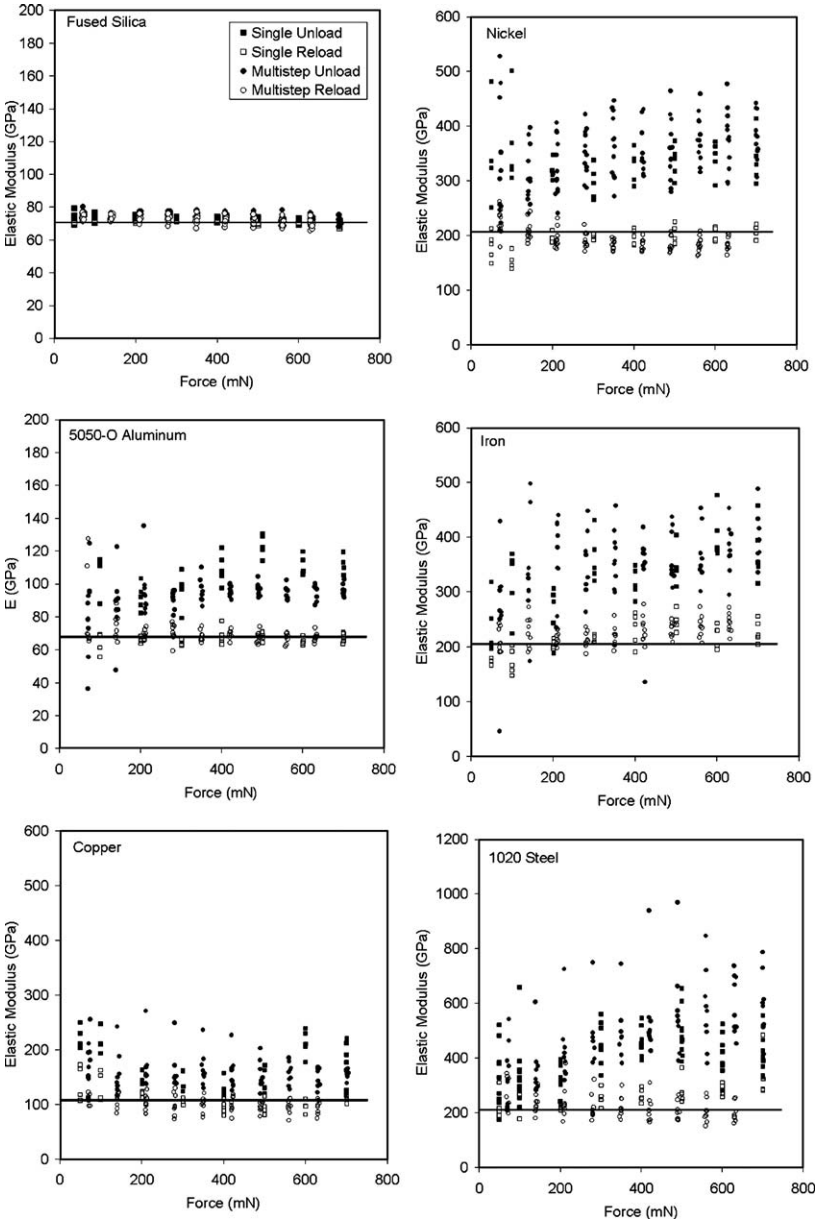

Fig. 5. The indentation elastic modulus for different materials from the unload (solid points) and reload (open points) curves obtained with the Shimadzu instrument at various applied force rates and hold times compared to the tensile test elastic modulus from reference literature (solid line) [12,13].

Table 1
A comparison of the unload and reload elastic modulus methods to the known tensile test elastic modulus for the tested materials [12,13]

Elastic modulus (GPa)	Fused silica	1020 steel	Nickel	Iron	5050-O aluminum	Copper
Tensile test	72	205	207	205	68.9	110
Unload	73.8± 1.89	449± 122	341± 57.0	342± 68.7	99.8± 12.5	166± 35.5
Reload	71.4± 2.02	244± 50.7	192± 20.7	219± 25.1	68.6±6.34	106± 18.7

time of 15 s also occurred at the minimum force for each step cycle, but low force creep was not observed.

Fig. 5 shows the elastic modulus for microindentation unload and reload curves obtained from load–unload–reload–unload and multistep tests at the various force rates and hold times. The dark lines in each of the graphs displayed in Fig. 5 are the tensile test elastic modulus taken from reference literature [12,13]. The unload curves for fused silica automatically produced correct results because the instrument frame-compliance and indenter projected area function were calibrated using fused silica. According to Pharr and Bolshakov [6], both the unloading and reloading processes are elastic, and what happens during reloading must be exactly the reverse of what happens during unloading. As predicted by these authors the reload curve elastic modulus results for fused silica were equivalent to the unload curve because it is a monolithic amorphous material. For the metals, in the force range between 50 and 100 mN, it was difficult to distinguish between the unload and reload curve elastic modulus results. However, as the force was increased to above 100 mN there was a clear separation between the elastic modulus calculated using the unload or reload curve. The fact that there is so much variation in the indentation results suggests uncertainty of the indentation methodology; therefore several tests must be done to take the average.

For the metals the unload elastic modulus increased as the force increased. On the other hand, as the reload curve was used the average elastic modulus were approximately equal to the tensile test elastic modulus, whether using load–unload–reload–unload or multistep procedure for various constant applied force rates and hold times. These tests indicated that when using the reload curve the force rate and hold time could be varied over a wide range with little influence on the elastic modulus calculation. In the case of aluminum, the average unload elastic modulus was 99.8±12.5 GPa that was much higher than the tensile test elastic modulus of 68.9 GPa [13]. However, the reload elastic modulus was correctly calculated as 68.6±6.34 GPa. As previously mentioned Garrido Maneiro and Rodríguez [4] also measured an increasing elastic modulus with an increasing force, for two other aluminum alloys.

Table 1 shows a comparison of the known tensile test elastic modulus to the average indentation elastic modulus from the unload and reload curve methods. It is observed for the metals that all the unload elastic modulus calculations were inaccurate while the reload elastic modulus was within one standard deviation of the tensile test elastic modulus. Aluminum had the least percentage difference between the unload and reload elastic modulus of 45%. The nickel and steel samples had the broadest percentage separation between the unload and reload elastic modulus, 78% and 84% respectively. Because of the multiphase or polycrystalline microstructure, the metals had a larger standard deviation as compared with fused silica.

Fig. 6 shows the load–unload–reload–unload curves for fused silica, copper, and steel obtained with the Nanoindenter XP for the same samples that were used with the Shimadzu DUH-W201S tester. The main difference between the two testers is that the Nanoindenter

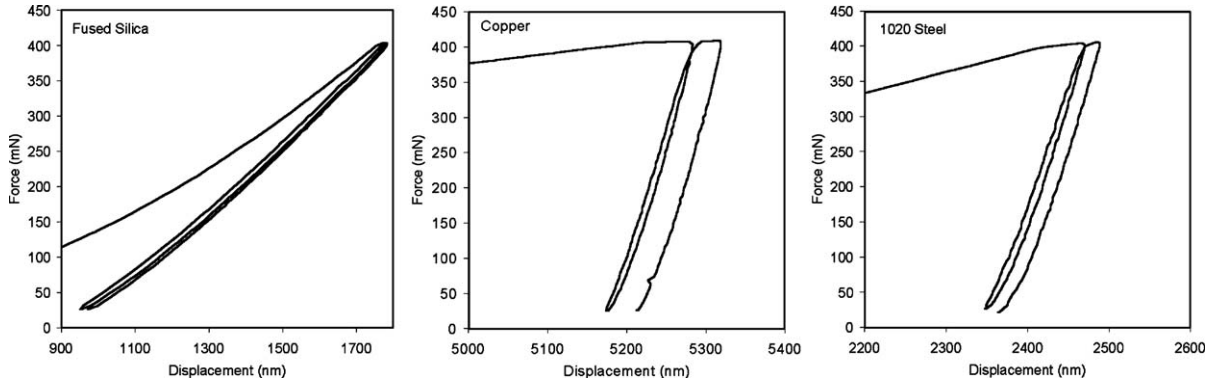

Fig. 6. The load–unload–reload–unload curve for the materials tested with the Nanoindenter XP instrument.

XP used a constant indentation displacement rate of 10 nm/s rather than a constant force rate. The metals in Fig. 6 are presented with the same displacement axis width of 400 nm and the fused silica displacement axis was set to 900 nm to accommodate for the large amount of elastic recovery. For the metals, the first and second unload curves appeared to have the same slope but were slightly offset because of the creep. For fused silica, the first and second unload curves appear to overlap. In general the reload curve presents a lower displacement than the unload curve forming a small hysteresis loop. In the present study the fused silica presented the smallest unload–reload loop whereas the metals showed a significantly wider space between the unload curves.

The metals reload curves started to deviate from the power law trend at between 80% and 100% of the previous maximum force. This deviation on the reload curve indicates the start of new plastic deformation (yielding). The fused silica showed no separation at the top of the reload curve, indicating that the maximum plastic deformation occurred on the initial loading.

Multistep tests were repeated for the fused silica and copper using the Nanoindenter XP (Fig. 7). This instrument measured the elastic modulus from the nanoscale into the microscale. Because this instrument was calibrated with fused silica, the unload curve results approximately equaled the known elastic modulus of 72 GPa at 75.6±1.81 GPa. The average was 3.6 GPa higher probably due to indenter tip wear. The reload elastic modulus was 74.0±1.70 GPa, a result that is again more close to the tensile test elastic modulus.

For copper a similar trend was observed, where the unload elastic modulus was slightly higher than the reload elastic modulus. The reload elastic modulus from the Nanoindenter XP was 111.7±10.5 GPa that is a value nearly that calculated from Shimadzu DUH-W201S of 106±18.7 GPa. However, below 5 mN, the

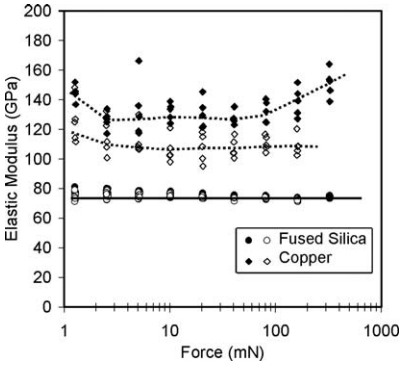

Fig. 7. The elastic modulus for fused silica and copper using the unload (solid) and reload (open) obtained with the Nanoindenter XP instrument.

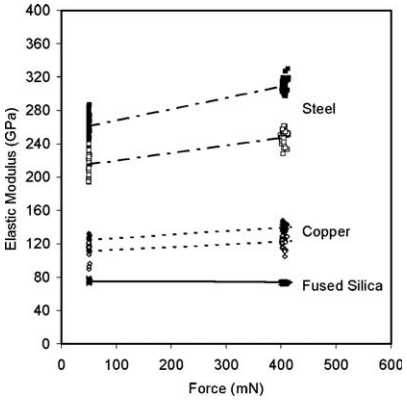

Fig. 8. The unload (solid) and reload (open) elastic modulus for 20 cycle indentation tests for three materials using the Nanoindenter XP instrument.

indent size effect was observed for both the unload and reload data. Above 100 mN, the copper unload elastic modulus began to increase with the increasing load while the reload elastic modulus remained constant, as previously observed for the other metals with Shimadzu ultra-micro hardness tester.

Fig. 8 shows the elastic modulus measured from a 20-cycle indentation test at 50 and 400 mN using the Nanoindenter XP for fused silica, copper, and steel. The indentation elastic modulus was measured for each of the 20 unload curves (solid data points) and the 19 reload curves (open data points). Again the fused silica presented the same resulting indentation elastic modulus (about 72 GPa) whether the unload or reload curve was used. On the other hand the metals presented a clear difference between the unload and reload elastic modulus. For the unload curve the copper and steel cycle tests were similar to the multistep tests showing an increasing elastic modulus with an increasing force. However, the reload method also indicated an increasing elastic modulus with displacement. This behavior was possibly caused by cold working during each cycle.

4. Discussion

We begin the discussion with an overview of the indentation process and an attempt to describe the reverse plasticity for metals. In the present study the Oliver–Pharr method for elastic modulus calculation was applied to both the unload and reload curves. Fused silica presented the same elastic modulus from the reload as the unload curve for all testing procedures. For the metals the difference in elastic modulus was insignificant in the force range of 1–100 mN. As the load was increased above 100 mN, the unload elastic modulus increased. In general

the reload curve method produced better elastic modulus results than the unload curve method. The value of reload elastic modulus was constant with increasing force and approximately equaled the tensile test elastic modulus value, presenting a small standard deviation.

The indentation behavior of the studied materials can be explained as follows. During the initial loading the material deforms as much elastically as plastically. At the top hold time, fused silica stops deforming plastically but the metals continue to creep (yield). The unloading starts at a constant force or displacement rate. During unloading, fused silica recovers elastically; however the metals display a mixture of elastic recovery and reverse plasticity. Oliver and Pharr [2] pointed out that the displacement recovery during the first unload may not be entirely elastic and, thus, the use of first unloading curves can sometimes lead to inaccuracies in the elastic modulus calculation. The present research found that, for metals, the additional reverse plasticity increased the slope of the unload curve and, therefore, increased the elastic modulus. Reverse plasticity in our opinion occurs due to internal stresses that are present in the material under load and that become "unstable" during unload. During unloading pinned dislocations relax, the grain boundary adjust, and even phase transition could occur which measurable changes the elastic modulus. The unload elastic recovery produces a different state of stress inside the material than the reload elastic deformation.

By using multistep tests, fused silica presented a constant elastic modulus, whether the unload or reload curve was used. In the case of the metals, the increasing unloading elastic modulus, as the load increased, indicate that the reverse plasticity influence also increased. On the other hand, the reloading behavior exhibited consistent elastic modulus results. For all materials tested the reload curve was at a slightly lower displacement and slope than the former unload curve, creating the commonly observed narrow hysteresis loop. It is believed that during initial reloading the material deforms elastically because the indenter already conforms to the residual indent impression shape. The contact area increases in a non-linear way because the sample elastic recovery is greatest in the indent center and least at the edge as predicted [6]. Fused silica displays a constant elastic deformation along the entire reload curve, but the metals started yielding at between 70% and 100% of the previous maximum force.

The reverse plasticity cannot be ignored when measuring the elastic modulus from indentation experiments. When the instrument is properly calibrated with fused silica the reverse plasticity behavior is clearly observed for metals at loads above 100 mN. Exactly what is reverse plasticity is yet to be determined. The elastic modulus for metals should be a measure of the atom-to-atom lattice spring constant. During unloading the stress relaxation is a dynamic process that involves more than just the crystal lattice elastic recovery. Reverse plasticity might be caused by dislocations, redistribution or grain boundary adjustments, or phase transitions reversion in order to reduce residual stress present in the sample, minimizing the energy of the bulk. These phenomena may be less significant during reloading. Another factor to consider is the contact between the indenter and sample, which might be better during reloading. This would provide a more homogeneous stress distribution. In any case, further research must be done to better understand reverse plasticity and its influence on the elastic modulus indentation calculation.

5. Conclusions

Two instrumented indentation testers with Berkovich indenters and several testing procedures were used to calculate the elastic modulus from the unload and reload curves using the Oliver–Pharr method. A number of conclusions were obtained from this research.

1. The fused silica, a monolithic amorphous material, was indifferent to either the unload or reload elastic modulus calculation.
2. For the metals the unload average elastic modulus was greater than the reload elastic modulus and increased with the increasing force. The reload method was within one standard deviation of the known tensile test elastic modulus for all tested materials.
3. Even when the force rate and the hold time varied over a broad range the results were reproducible. The two instrumented indentation testers presented similar results from the nanoscale into the microscale.
4. The unload curve analysis provides good results for the monolithic materials like fused silica. In the case of metals, the unload method worked well below 100 mN. Above 100 mN reverse plasticity appears to cause an error in the unload elastic modulus calculation for metals.
5. The reload curve analysis procedure could be used to calculate the elastic modulus of both monolithic materials and polycrystalline metals from nanoscale to microscale loads.

Acknowledgements

The authors thank the Brazilian institutions FAPEMIG and CNPq for financial support. David J. Shuman is

thankful to the TIB program/CNPq and André L.M. Costa is thankful to the Instituto do Milênio de Nanociências/CNPq for research grants. We also thank Professor Carlos M. Lepienski from the Universidade Federal do Paraná-Brazil, for technical assistance and commentaries on the manuscript, and Mr. Fabrício F. Cardoso for laboratory testing.

References

[1] Doerner MF, Nix WD. A method for interpreting the data from depth-sensing indentation instruments. J Mater Res 1986;1:601–9.
[2] Oliver WC, Pharr GM. An improved technique for determining hardness and elastic modulus using load and displacement sensing indentation measurements. J Mater Res 1992;7:1564–83.
[3] Rodríguez R, Gutierrez I. Correlation between nanoindentation and tensile properties influence of the indentation size effect. Mater Sci Eng 2003;A361:377–84.
[4] Garrido Maneiro MA, Rodríguez J. Pile-up effect on nanoindentation tests with spherical–conical tips. Scr Mater 2005;52:593–8.
[5] Sargent PM, Page TF. The possible effects of elastic recovery on the microhardness of anisotropic materials. Scr Metall 1981;15:245–50.
[6] Pharr GM, Bolshakov A. Understanding nanoindentation unloading curves. J Mater Res 2002;17(10):2660–71.
[7] Gogotsi YG, Domich V, Dub SN, Kailer A, Nickel KG. Cyclic nanoindentation and Raman microspectroscopy study of phase transformations in semiconductors. J Mater Res 2000;15(4):871–9.
[8] Fisher-Cripps AC. Nanoindentation, vol. 1. Berlin: Springer; 2002. p. 2–16.
[9] Hay JL, Pharr GM. ASM handbook mechanical testing and evaluation. In: Kuhn H, Medlin D, editors. 10th ed. Materials Park, OH: ASM International; 2000. p. 232–43.
[10] Oliver WC, Pharr GM. Measuring of hardness and elastic modulus by instrumented indentation: advances in understanding and refinement of methodology. J Mater Res 2004;19 (1):3–20.
[11] Lepienski CM, Foerster CE. Nanomechanical properties by nanoindentation. In: Nalwa HS, editor. Encyclopedia of nanoscience and nanotechnology, vol. 7. American Scientific; 2004. p. 1–20.
[12] Metals, Handbook, Vol. 1. Properties and selection: irons, steels, and high-performance alloys. 10th ed. ASM International; 1990.
[13] Metals Handbook, Vol. 2. Properties and selection: nonferrous alloys and special-purpose materials. 10th ed. ASM International; 1990.